JOURNAL OF APPLIED ELECTROCHEMISTRY **25** (1995) 126–136

Mechanism of anodic oxidation of chlorate to perchlorate on platinum electrodes

L. J. J. JANSSEN, P. D. L. VAN DER HEYDEN

Faculty of Chemical Engineering, Eindhoven University of Technology, PO Box 513, 5600 MB Eindhoven, The Netherlands

Received 15 February 1994; revised 20 June 1994

The kinetics and mechanism of the anodic oxidation of chlorate to perchlorate on platinum electrodes have been investigated. The current efficiency for perchlorate formation and the electrode potential have been determined as a function of current density for various solution compositions, flow rates and pHs at 50° C. The results have been compared with theoretical relations between the ratio of the current efficiencies for perchlorate and oxygen formation, the electrode potential, the concentration of chlorate at the electrode surface and the current density for various possible mechanisms. It is concluded that the formation of an adsorbed hydroxyl radical is the first step in the overall electrode reaction. The mechanism proposed for the ClO_4 perchlorate and oxygen formation is:

$$H_2O \longrightarrow (OH)_{ad} + H^+ + e^-$$

$$ClO_3^- + (OH)_{ad} \longrightarrow ClO_4^- + H^+ + e^-$$

$$2(OH)_{ad} \longrightarrow O_{ad} + H_2O$$

$$2O_{ad} \rightleftharpoons O_2$$

The ratio between the current efficiency for perchlorate and that for oxygen formation is determined by the rate of the electrode reaction involving ClO_3^- and that for the combination reaction of $(OH)_{ad}$.

List of symbols

A_e	electrode surface area (m^2)
b	Tafel slope (mV)
c	concentration of chlorate in kmol per m^3 solution (M or molarity) ($kmol\,m^{-3}$) or in mol chlorate per kg of water (m or molality) ($kmol\,kg^{-1}$)
c_b	c in the bulk of the solution ($kmol\,m^{-3}$ or $mol\,kg^{-1}$)
c_s	c at the electrode surface ($kmol\,m^{-3}$ or $mol\,kg^{-1}$)
E	electrode potential vs SCE (V)
E_m	measured potential between working electrode reference electrode (V)
E_r	reversible electrode potential (V)
E_r^*	reference electrode potential (V)
E_Ω	ohmic potential drop (V)
F	Faraday constant ($C\,mol^{-1}$)
f	F/RT (V^{-1})
i	current density ($A\,m^{-2}$ or $kA\,m^{-2}$)
i_i	i for the production of species i ($A\,m^{-2}$)
I	current (A)
k_i	chemical reaction rate constant for reaction i ($m\,s^{-1}$)
k_i^e	electrochemical reaction rate constant at the reference potential for reaction i ($m\,s^{-1}$)
k_i^m	mass transfer coefficient for species i ($m\,s^{-1}$)
$k_{B,i}^m$	k_i at gas evolution and in the absence of forced convection ($m\,s^{-1}$)
$k_{F,i}^m$	k_i at forced convection ($m\,s^{-1}$)
$k_{FB,i}^m$	k_i at a combination of forced and bubble induced convention ($m\,s^{-1}$)
m	molality
p_1	parameter in Fig. 11
p_2	parameter in Figs 12 and 13
q	slope of $\log p_2/\log c_s$ curve
R	gas constant ($J\,mol^{-1}\,K^{-1}$)
R_Ω	ohmic resistance (Ω)
T	absolute temperature (K)
u_s	rate of solution flow ($m\,s^{-1}$)
v_i	rate of reaction i ($mol\,s^{-1}\,m^{-2}$)

Greek letters

α	anodic transfer coefficient (–)
α_i	α for reaction i (–)
Γ	current efficiency (–)
Γ_i	Γ for the production of species i (–)
η	$E - E_R$ (V)
θ_i	fractional coverage of the electrode by species i (–)

0021-891X

1. Introduction

The most common industrial method of producing perchlorate is the electrochemical oxidation of aqueous chlorate solutions [1]. The anode material is crucial to obtain a high current efficiency for the perchlorate formation. Only two materials, viz. smooth platinum and lead dioxide are used industrially [1]. The current efficiency for perchlorate formation at a platinum anode is clearly the highest [2, 3].

Mechanisms for the anodic chlorate oxidation on platinum or lead dioxide anodes have been proposed in the literature. Recently, a review of the kinetics mechanism of perchlorate formation has been published [4]. Most of the mechanisms suggested in previous literature are based on indirect or inadequate experimental support [4]. Munichandraiah and Sathyanarayana [4] have shown that the most probable mechanism involves the oxidation of a water molecule in a one-electron transfer step to give an adsorbed hydroxyl radical as the rate-determining step for the overall reaction. After the first step, they have proposed two possible reaction schemes. However, since the perchlorate formation is strongly kinetically hindered there may be significant differences between the mechanisms on Pt and PbO_2, a thorough study for a platinum anode is therefore required. Moreover, some experimental data on current efficiency and anode potential are open to discussion. The effect of a number of parameters on the current efficiency for perchlorate formation has been determined in the present work.

2. Reaction at the anode

Chlorate is oxidized anodically to perchlorate according to the overall reaction:

$$ClO_3^- + H_2O \longrightarrow ClO_4^- + 2H^+ + 2e^- \quad (1)$$

The standard potential of this reaction $E^0 = 0.95$ V vs SCE and is close to that of the oxidation of water, viz. $E^0 = 0.99$ V:

$$2H_2O \longrightarrow O_2 + 4H^+ + 4e^- \quad (2)$$

Only oxygen and perchlorate are formed at the anode during electrolysis under the conditions used in this investigation [5]. In this case the sum of the current efficiencies Γ_{O_2} and Γ_{ClO_4} is equal to 1. The formation of ozone can only take place under extreme electrolysis conditions like high current density and low chlorate concentration.

3. Experimental details

3.1. *Equipment*

The experimental setup with two separate solution circuits is shown in Fig. 1. The electrolysis cell has been described previously [6, 7]. The anodic and cathodic compartment of the cell were separated by a cation-exchange membrane (Nafion®117). The

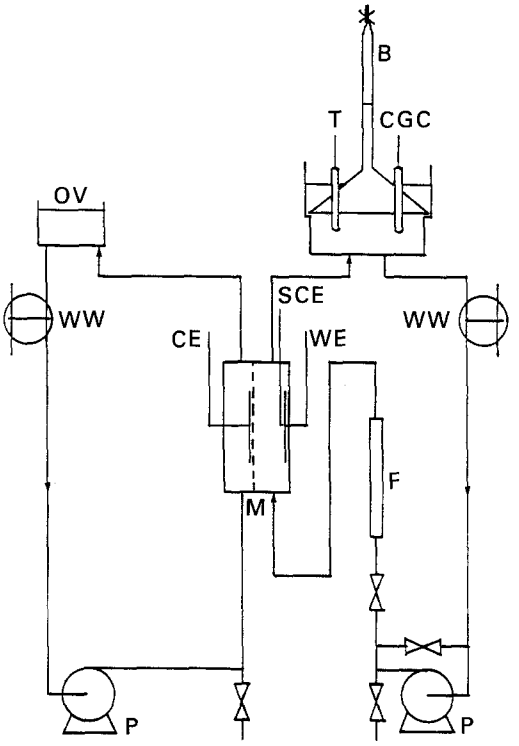

Fig. 1. Experimental setup. WE: working electrode (anode), CE: counter electrode (cathode), M: membrane, SCE: saturated calomel electrode, CGC: combined glass-calomel electrode, T: automatic titrator, OV: overflow vessel, B: bell with burette to collect gas, P: pump, WW: heat exchanger, F: flowmeter.

working electrode was a smooth platinum sheet, 76.4 mm in length and 10.0 mm in width, unless otherwise stated. Its geometric surface area was 764 mm^2. In some cases, a shorter electrode was used in order to obtain a high current density when the potential–current measurements were carried out. The counter electrode was a perforated nickel plate with the same geometric dimensions as the standard working electrode.

A Luggin capillary was placed in a hole located in the middle of the working electrode. This capillary was filled with a solution with the same composition as the anolyte at the start of the electrolysis and was connected to a saturated calomel electrode (SCE), which was used as the reference electrode. A piece of Nylon cloth was inserted into the capillary to prevent entry of gas bubbles.

The electrolyses were carried out galvanostatically, using a power supply (Delta Elektronika, type D050-10) at 50° C. The potential between the working electrode and the reference electrode was registered by a recorder and this potential was corrected for the ohmic potential drop. All potentials stated are relative to the potential of the saturated calomel electrode (SCE). Polarization curves obtained by adjustment of the current were called galvanostatic polarization curves.

Two experimental methods were used to determine the ohmic potential drop, viz. the current interruption technique and a.c. impedance spectroscopy. For the first method the current was switched off using a mercury relay (Eliott EB 1541) and the resulting

potential decay was registered on a storage oscilloscope. The registration time scale was 20 ms cm^{-1}.

A.c. impedance spectroscopy was carried out with a Solartron 1250 frequency response analyser and a Solartron electrochemical interface 1286, coupled with a HP microcomputer. This combination of apparatus was also used to measure the relation between current and potential. The potential was varied at a scan rate of 5 mV s^{-1} between a minimum and a maximum value to give a potentiodynamic polarization curve. To maintain the pH of the anolyte constant during the electrolysis, viz pH 10, an alkaline solution was added to the anolyte. The addition of the alkaline solution was regulated by an automatic titrator (Radiometer, type TTTiC), a valve and a burette. The alkaline solution was a solution with the composition of the initial anolyte to which solid NaOH had been added to yield a 4 M NaOH concentration.

To obtain the rate of oxygen formation during electrolysis, the anodic oxygen gas was collected by a bell hanging in the overflow vessel with an inner diameter of 180 mm. The bell consisted of a 50 cm^3 burette and a tunnel with an outer diameter slightly smaller than the inner diameter of the overflow vessel. The bell was placed on a shelf on the inner port of the overflow vessel. Both the burette and the overflow vessel were thermostated.

Usually, the time to collect 10 cm^3 anodic gas in the same part of the burette was determined using a stopwatch. To determine whether loss of anodic oxygen gas occurred, electrolyses were carried out with a 1 M NaOH solution as the anolyte. In this case the current efficiency for the oxygen formation was assumed to be 1. It was found that no oxygen losses occurred. Perchlorate formation current efficiency was calculated by subtracting the oxygen formation current efficiency from 1.

4. Results

Preliminary experiments showed that the history of a platinum anode strongly affects the current efficiency for perchlorate formation. A remarkable result is presented in Fig. 2 for an almost unused platinum electrode.

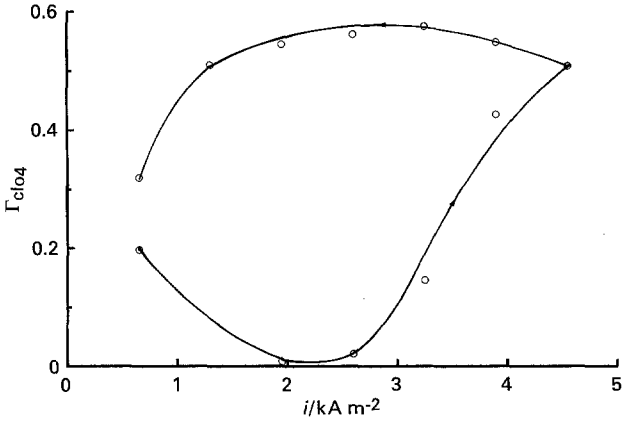

Fig. 2. Perchlorate current efficiency as a function of current density for an almost unused platinum anode in 0.47 *m* $NaClO_3$, at a solution flow rate of 0.06 m s^{-1}, 50° C and at pH 10. The series of experiments was started at $i = 0.70$ kA m^{-2}. The arrow indicates the direction of the change in the applied current density.

To obtain reproducible results, anode prepolarization was found to be indispensable. This prepolarization was carried out at potentials where perchlorate was formed. The prepolarization time required to obtain reproducible results depends strongly on the history of the platinum anode and varied from some hours for an almost new anode to some minutes for an anode used many times with short intervals. It was found that the history of the electrode has a much larger effect on the current efficiency than on the anode potential. This means that the current efficiency for perchlorate is more sensitive to changes in the condition of the platinum electrode surface than the anode potential.

4.1. *Polarization curves*

The industrial production of perchlorate takes place at high current densities (i.e., higher than 1 kA m^{-2}). To obtain a true anodic polarization curve, correction for the ohmic potential drop, E_Ω, between the Luggin tip and the working electrode is necessary. It was found that the potential decay curve showed an insufficiently sharp change in slope during the first 20 ms, so that the use of the current interruption method was questionable. The experimental ohmic potential drop obtained by the interruption method increased linearly with current density. However, this was evidently too high (about 20%) since the resulting polarization curve was overcompensated especially at high current densities. The ohmic resistance R_Ω between the tip of the Luggin capillary and the working electrode was also determined by the a.c. technique. The experimental Argand diagrams, especially at high current densities, did not show well formed semicircles. Correct extrapolation in the high frequency range was very difficult and practically impossible. Probably, Munichandraiah and Sathyanarayana [4] experienced similar problems in determining the ohmic potential drop correctly. They have estimated E_Ω from their experimental $E_m/\ln i$ curve assuming that the ohmic resistance $R_\Omega = E_\Omega/I$ is constant and E increases linearly with increasing $\ln i$. This method was adopted to calculate the ohmic potential drop in this work.

Since $E_m = E + R_\Omega I$ and $i = I/A_e$ and assuming the anode potential can be written as $E = a + b \ln i$, it can be deduced that

$$\frac{dE_m}{dI} = R_\Omega + \frac{b}{I} \qquad (3)$$

Anodic polarization curves on smooth platinum electrodes in $NaClO_3$ solutions show a strong inflection [5]. This means that the adopted method to calculate the ohmic potential drop must be used carefully. To show the inflection in a polarization curve, this curve is given for a wide potential range corrected for the ohmic potential drop for three different

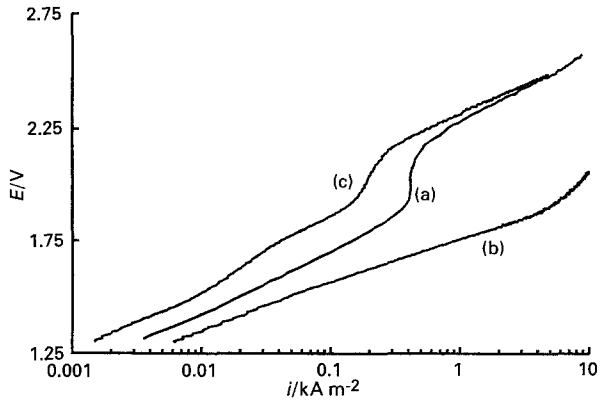

Fig. 3. Potentiodynamic polarization curves for a platinum anode in various solutions and at 50° C. Potential scan rate is $5\,mV\,s^{-1}$. (a) $3.76\,m$ $NaClO_3$, (b) $1.64\,m$ $NaClO_4$ and (c) $3.76\,m$ $NaClO_3 + 1.64\,m$ $NaClO_4$.

solutions, viz. $3.76\,m$ $NaClO_3$, $1.64\,m$ $NaClO_4$ and $3.76\,m$ $NaClO_3 + 1.64\,m$ $NaClO_4$. These curves were measured at a potential-scan rate of $5\,mV\,s^{-1}$ in the cathodic direction. The $E/\log i$ curves show two ranges of behaviour for solutions containing $3.76\,m$ $NaClO_3$ (Fig. 3). The first stage, occurring between 1.3 and 1.9 V, was found to correspond to oxygen evolution and the second stage, higher than 2.2 V, corresponded to perchlorate formation [5]. In the transition range from 1.9 to 2.2 V, the nature of the anode surface may change strongly. For experiments at very high current efficiency for chlorate formation, it is likely that the Tafel slope will be practically constant.

Constant-current electrolysis with a high concentration of $NaClO_3$ (i.e., $3.76\,m$ $NaClO_3$) at current densities from 0.5 to $5\,kA\,m^{-2}$ and with a high flow-rate of solution, viz. $0.33\,m\,s^{-1}$, satisfies the conditions for use of the calculation method for the ohmic potential drop, since, under these electrolysis conditions, the concentration polarization for chlorate is practically zero and the current efficiency for perchlorate formation is high (i.e. > 0.95). Figure 4 shows galvanostatic polarization curves for a prepolarized electrode in a solution with a high chlorate concentration and at various flow rates. The ohmic resistance R_Ω was calculated from the E_m/I curve at the highest rate of flow (i.e., $u_s = 0.33\,m\,s^{-1}$) using the method described above. It was found that R_Ω at $u_s = 0.33\,m\,s^{-1}$ agreed with the value determined by the a.c. technique, when the inaccuracy in the experimental results was taken into account. Assuming R_Ω reaches a constant value at $u_s = 0.33\,m\,s^{-1}$. R_Ω at this flow rate of solution was used to calculate E_Ω at lower rates of flow.

To obtain reliable polarization curves for a solution with a low concentration of $NaClO_3$, R_Ω for this solution was determined from R_Ω for the highest $NaClO_3$ concentration where the difference in the solution electric conductivities was taken into account. Direct application of this method to calculate R_Ω for solutions with a low $NaClO_3$ concentration is incorrect, because of the occurrence of concentration polarization. Figure 5 shows the electrode potential as a function of current density for solutions with $1.64\,m$ $NaClO_4$ and various concentrations of $NaClO_3$.

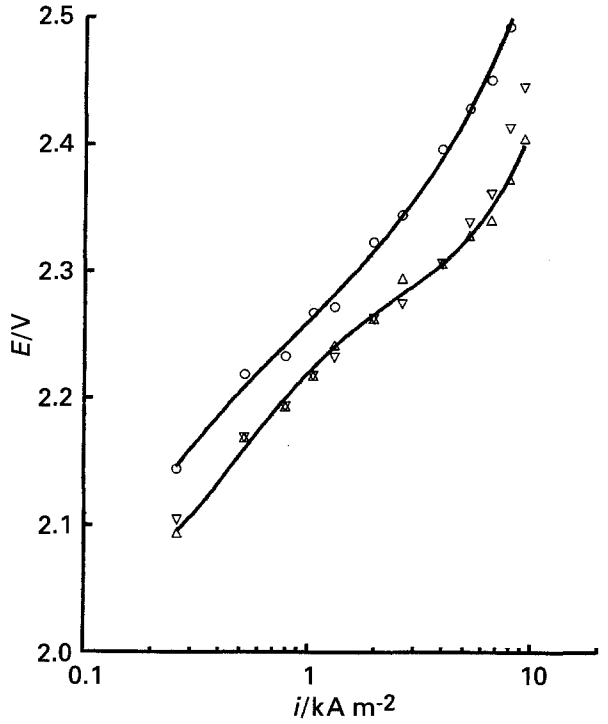

Fig. 4. Galvanostatic polarization curves for a platinum anode in a $3.76\,m$ $NaClO_3 + 1.64\,m$ $NaClO_4$ solution at various solution flow rates u_s and at 50° C. Key: (○) $u_s = 0.06\,m\,s^{-1}$, (▽) $u_s = 0.24\,m\,s^{-1}$ and (△) $u_s = 0.33\,m\,s^{-1}$.

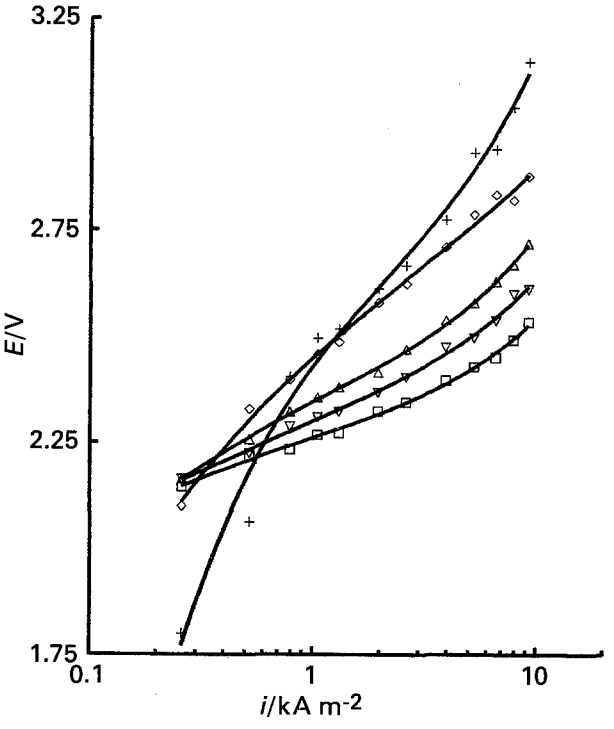

Fig. 5. Galvanostatic polarization curves for a platinum anode in solutions containing $1.64\,m$ $NaClO_4$ and various concentrations of $NaClO_3$, at a solution-flow rate of $0.06\,m\,s^{-1}$ and at 50° C. $NaClO_3$ concentrations: Key: (+) $0.038\,m$, (◇) $0.47\,m$, (△) $0.94\,m$, (▽) $2.35\,m$ and (□) $3.76\,m$.

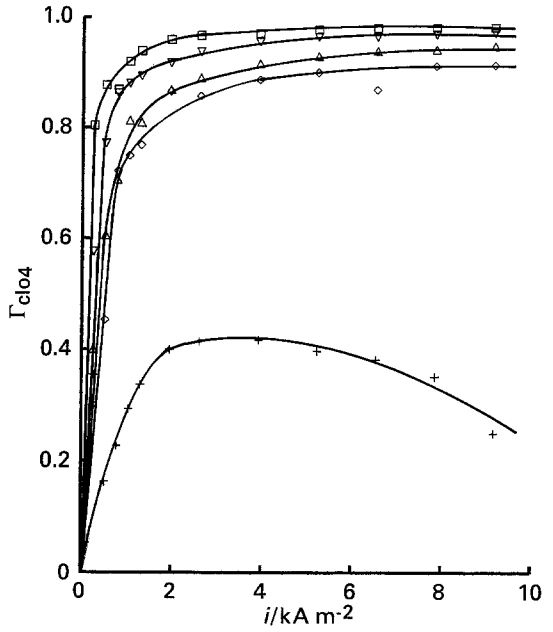

Fig. 6. Perchlorate current efficiency as a function of current density for a platinum anode in solutions containing 1.64 m $NaClO_4$ and various concentrations of $NaClO_3$ and at a solution-flow rate of 0.06 m s^{-1} and 50° C. $NaClO_3$ concentrations: (+) 0.038 m, (◇) 0.47 m, (△) 0.94 m, (▽) 2.35 m and (□) 3.76 m.

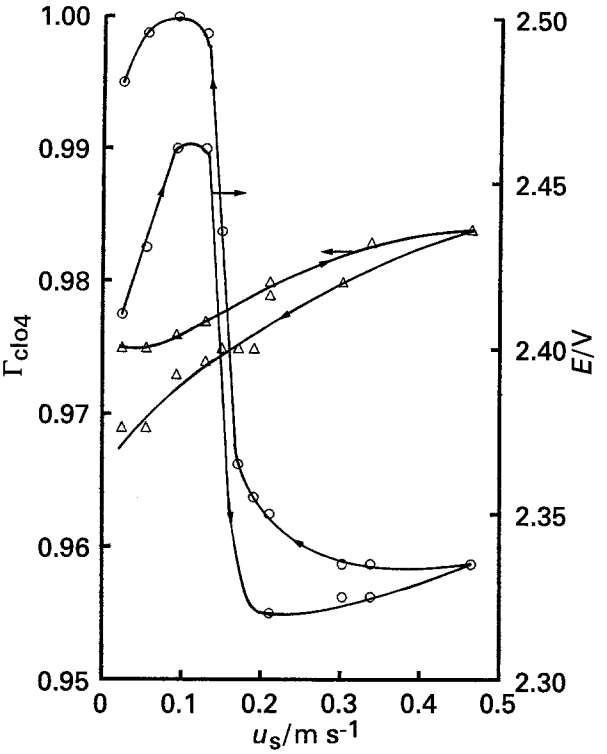

Fig. 7. Perchlorate current efficiency (△) and electrode potential (○) as a function of solution flow rate for a platinum anode in a 4.69 m $NaClO_3$ solution at a current density of 6.55 kA m^{-2} and at 50° C. The arrows on the curves indicate the direction of the change in the flow rate of solution.

4.2. *Current efficiency*

The current efficiency for perchlorate formation, Γ_{ClO_4} is $1 - \Gamma_{O_2}$. The perchlorate current efficiency shown was found for a platinum electrode prepolarized for a sufficiently long period to obtain constant results. To determine the mass transfer coefficient for chlorate, as a function of the rate of oxygen evolution, electrolyses were carried out for $NaClO_3$–$NaClO_4$ solutions with a low $NaClO_3$ concentration. These results will be published separately.

Figure 6 shows the effect of the chlorate concentration on the relation between the perchlorate current efficiency and the current density for a platinum electrode in $NaClO_3$–$NaClO_4$ solutions with various concentrations of $NaClO_3$. The electrode potentials for these experiments are given in Fig. 5. From Fig. 6 it follows that the perchlorate current efficiency increases with increasing $NaClO_3$ concentration and increasing current density with the exception of experiments conducted with 0.038 m $NaClO_3$-solution. Moreover, the perchlorate current efficiency approaches zero at current densities approaching zero.

The effect of solution flow rate on perchlorate current efficiency for a platinum anode in a 4.69 m $NaClO_3$ is shown in Fig. 7. The electrode potential is also given in this Figure.

The effect of the solution flow rate on the relation between perchlorate current efficiency and current density for a platinum anode in a 3.76 m $NaClO_3$ + 1.64 m $NaClO_4$ solution is shown in Fig. 8. The electrode potentials corresponding to these experiments are given in Fig. 4.

The effect of the pH was determined for $NaClO_3$ solutions with various concentrations, i.e., 0.28 and 4.70 M. The other conditions of electrolysis were $T = 323$ K, $u_s = 0.06$ m s^{-1} and $i = 3.24$ kA m^{-2}. It was found that the current efficiency for perchlorate formation does not depend on pH for the investigated pH range from 2 to 11. The current efficiencies

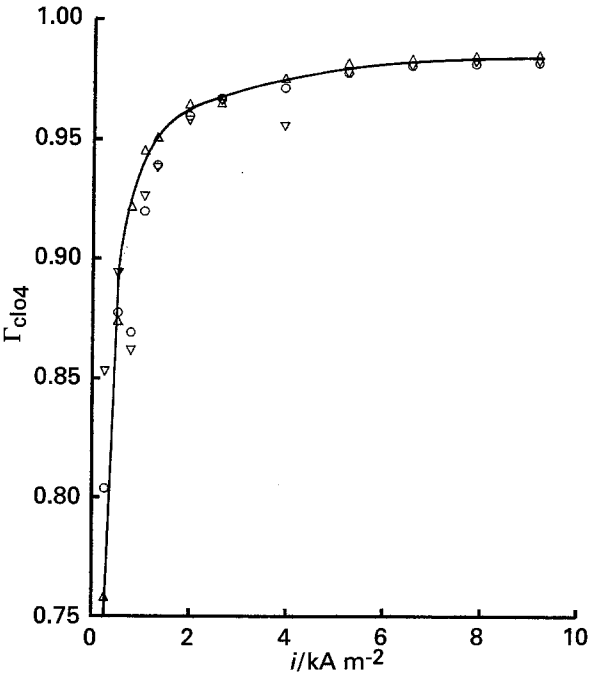

Fig. 8. Perchlorate current efficiency as a function of current density for a platinum anode in a 3.76 m $NaClO_3$ + 1.64 m $NaClO_4$ solution at 50° C and at various rates of solution flow. Solution flow rates: (▽) 0.06 m s^{-1}, (△) 0.24 m s^{-1} and (○) 0.33 m s^{-1}.

for perchlorate formation were 0.69 and 0.92 for 0.28 and 4.70 *m* $NaClO_3$, respectively.

5. Theory

5.1. *Mechanisms for perchlorate formation*

Several mechanisms for the anodic oxidation of chlorate to perchlorate in aqueous media have been proposed in the literature [4]. During electrolysis of a $NaClO_3$–$NaClO_4$ solution under industrial conditions the pH of the solution at the perchlorate producing anode is very low. Consequently, the mechanisms involving OH^- ions are not taken into consideration.

To elucidate the mechanism for perchlorate formation, an important question will be the possible participation of the intermediates $(OH)_{ads}$ or $(O)_{ads}$ formed by water discharge. Hydroxyl radicals adsorbed on the platinum anode are produced by the discharge of H_2O in acid-solution [8]

$$(H_2O)_{ads} \xrightarrow{\text{slow}} (OH)_{ads} + H^+ + e^- \qquad (4)$$

as the rate-determining step. This step is followed either by the fast combination of OH radicals,

$$(OH)_{ads} + (OH)_{ads} \longrightarrow (O)_{ads} + H_2O \qquad (5)$$

or by the discharge of OH radicals

$$(OH)_{ads} \rightleftharpoons (O)_{ads} + H^+ + e^- \qquad (6)$$

to produce adsorbed O atoms. Finally, oxygen is evolved by the rapid combination of adsorbed atoms

$$(O)_{ads} + (O)_{ads} \rightleftharpoons (O_2)_{ads} \qquad (7)$$

followed by desorption of the adsorbed O_2 molecules

$$(O_2)_{ads} \rightleftharpoons O_2 \qquad (8)$$

Above the limiting current region, that is, the transition from the lower to the upper Tafel region, the evolution of oxygen takes place on the catalytically stable layer of Pt–O or PtO_2 [8]. This Pt–O or PtO_2 does not participate in the electrode reaction but acts only as the catalytic surface on which oxygen evolution proceeds [9]. Recently, it has been established that a platinum anode in 0.5 *m* H_2SO_4 at potentials in the upper Tafel region is covered by an oxidation layer consisting of $Pt(OH)_4$ [10]. Since the pH of the solution at the perchlorate producing platinum anode is very low, it is likely that this platinum anode is also covered by $Pt(OH)_4$. The current efficiency for perchlorate formation is practically constant in the pH range from 2 to 11 (Section 4.2). Consequently, the nature of the electrode surface does not depend on the pH of the bulk solution in the pH range from 2 to 11.

Oxygen atoms will be present on the surface of the platinum anode over the whole range of potentials, where oxygen evolution occurs (Fig. 4). The formation of perchlorate does not occur at potentials in the lower Tafel region, but occurs at a detectable rate at potentials in the upper Tafel region.

The platinum anode at potentials in the upper Tafel region is covered by a $Pt(OH)_4$ layer. The fractional coverage of this layer by oxygen atoms is very low and increases with increasing potential.

Table 1. Possible mechanisms for perchlorate formation

Mechanism	*Mechanism steps**			
I	H_2O	$\rightarrow$	$(OH)_{ads} + H^+ + e^-$	(a)
	ClO_3^-	$\rightarrow$	$(ClO_3)_{ads} + e^-$	(b)
	$(ClO_3)_{ads} + H_2O$	$\rightleftharpoons$	$HClO_4 + H^+ + e^-$	(c)
	$HClO_4$	$\rightleftharpoons$	$ClO_4^- + H^+$	(i)
	$(OH)_{ads}$	$\rightleftharpoons$	$O_{ads} + H^+ + e^-$	(e)
	$2(O)_{ads}$	$\rightleftharpoons$	O_2	(f)
II	H_2O	$\rightarrow$	$(OH)_{ads} + H^+ + e^-$	(a)
	ClO_3^-	$\rightarrow$	$(ClO_3)_{ads} + e^-$	(b)
	$(ClO_3)_{ads} + (OH)_{ads}$	$\rightleftharpoons$	$ClO_4^- + H^+$	(d)
	$(OH)_{ads}$	$\rightleftharpoons$	$O_{ads} + H^+ + e^-$	(e)
	$2(O)_{ads}$	$\rightleftharpoons$	O_2	(f)
III	H_2O	$\rightarrow$	$(OH)_{ads} + H^+ + e^-$	(a)
	$ClO_3^- + (OH)_{ads}$	$\rightarrow$	$ClO_4^- + H^+ + e^-$	(g)
	$(OH)_{ads}$	$\rightarrow$	$(O)_{ads} + H^+ + e^-$	(e)
	$2(O)_{ads}$	$\rightleftharpoons$	O_2	(f)
IV	H_2O	$\rightarrow$	$(OH)_{ads} + H^+ + e^-$	(a)
	$ClO_3^- + (OH)_{ads}$	$\rightarrow$	$ClO_4^- + H^+ + e^-$	(g)
	$2(OH)_{ads}$	$\rightarrow$	$(O)_{ads} + H_2O$	(h)
	$2(O)_{ads}$	$\rightleftharpoons$	O_2	(f)

* Two arrows indicate a kinetically reversible (i.e., fast) step.

Mechanisms with a two-electron step as the rate-determining step are very unlikely [8] and excluded. Therefore, it is assumed that adsorbed oxygen atoms are formed by two successive reactions, Reactions 4 and 5 or 6, and perchlorate ions are formed according to:

$$ClO_3^- + O_{ad} \longrightarrow ClO_4^- \qquad (9)$$

Since molecular oxygen is formed by a combination of adsorbed oxygen atoms according to Reaction 7, and the degree of coverage by oxygen atoms increases with increasing potential, it can be shown that the ratio $\Gamma_{ClO_4}/\Gamma_{O_2}$ decreases with increasing potential. However, from Fig. 6 it follows that $\Gamma_{ClO_4}/\Gamma_{O_2}$ increases strongly with increasing potential. Perchlorate mechanisms involving O_{ad} were taken into consideration and had to be excluded.

Possible mechanisms for the anodic oxidation of a ClO_3^- ion to a ClO_4^- ion and their steps are shown in Table 1. Moreover, steps for oxygen evolution are also tabulated when they may be relevant for perchlorate formation. For each mechanism Table 1 shows the probable rate-determining step indicated by one arrow, while two arrows indicate the fast step.

5.2. *Current efficiency relations for selected mechanisms*

Valuable information characterising the mechanism of the perchlorate formation can be obtained from the ratio between the perchlorate and oxygen current efficiency. To simplify the equations for the reaction rates, it is assumed that the fractional coverages for the reacting intermediates are very small viz. $\theta_i \ll 1$

and the rate of the backward reaction is negligible. Moreover, a reference electrode potential, E_R, is introduced to correlate the various rate equations. The difference $E - E_R$ is denoted by η. The reversible electrode potential $E^*_{r,1}$ at $c_b = 1\,\text{kmol}\,\text{m}^{-3}$ for the redox reaction $ClO_3^- + H_2O \rightleftharpoons ClO_4^- + 2H^+ + 2e^-$ is chosen as the reference electrode potential. From the definition of the reversible electrode potential, $E_{r,1}$, it follows that:

$$E_{r,1} = E^*_{r,1} - (2f)^{-1} \ln c_b \qquad (10)$$

where the concentrations for H_2O, ClO_4^- and H^+ are considered to be constant.

5.2.1. Mechanism I. The rate of (b) is given by

$$v_b = k_b^e c_s \exp(\alpha_b f \eta) \qquad (11)$$

and that of (a) by

$$v_a = k_a^e \exp(\alpha_a f \eta) \qquad (12)$$

Since $i_b = Fv_b$, $i_a = Fv_a$, $i_{ClO_4} = 2i_b$, $i_{O_2} = 4i_a$ and $i = i_{O_2} + i_{ClO_4}$ it is deduced that the ratio of the current densities or the current efficiencies for perchlorate and oxygen is

$$\frac{i_{ClO_4}}{i_{O_2}} = \frac{\Gamma_{ClO_4}}{\Gamma_{O_2}} = \frac{k_b^e}{2k_a^e} c_s \exp\{(\alpha_b - \alpha_a) f \eta\} \qquad (13)$$

It can be shown that the Tafel slopes of the $\eta/\ln i_a$ and $\eta/\ln i_b$ curves are $(\alpha_a f)^{-1}$ and $(\alpha_b f)^{-1}$, respectively, where $i_a = 0.25 i_{O_2}$ and $i_b = 0.5 i_{ClO_4}$.

5.2.2. Mechanism II. At steady state

$$v_b = v_d \qquad (14)$$

and

$$v_a = v_d + v_e \qquad (15)$$

The rate equation for (a) is given by Equation 12, for (b) by Equation 11, for (d) by

$$v_d = k_d \theta_{ClO_3} \theta_{OH} \qquad (16)$$

and for (e) by

$$v_e = k_e^e \theta_{OH} \exp(\alpha_e f \eta) \qquad (17)$$

From Equation 11 and Equations 14–17 it follows

$$\frac{v_d}{v_d + v_e} = \frac{k_b^e c_s}{k_a^e} \exp\{(\alpha_b - \alpha_a) f \eta\} \qquad (18)$$

Since $i_a = Fv_a$, $i_b = Fv_b$ and $i_e = Fv_e$ it follows that

$$i_{O_2} = 4i_e = 4Fv_e \qquad (19)$$

and

$$i_{ClO_4} = 2i_b = 2Fv_b = 2Fv_d \qquad (20)$$

The ratio of current efficiencies for perchlorate and oxygen is

$$\Gamma_{ClO_4}/\Gamma_{O_2} = i_{ClO_4}/i_{O_2} = \frac{v_d}{2v_e} \qquad (21)$$

From Equations 21 and 18 it follows that

$$\frac{2\Gamma_{ClO_4}}{2\Gamma_{ClO_4} + \Gamma_{O_2}} = \frac{k_b^e c_s}{k_a^e} \exp\{(\alpha_b - \alpha_a) f \eta\} \qquad (22)$$

For mechanism II it follows that (a) and (b) are parallel reactions. Each reaction can be the rate-determining step. It can be shown that the Tafel slopes of the $\eta/\ln i_a$ and $\eta/\ln i_b$ curves are $(\alpha_a f)^{-1}$ and $(\alpha_b f)^{-1}$ for (a) and (b), respectively, as the rate determining step, and where

$$i_a = i - \tfrac{1}{2} i_{ClO_4} - \tfrac{3}{4} i_{O_2} \quad \text{and} \quad i_b = \tfrac{1}{2} i_{ClO_4} \qquad (23/24)$$

5.2.3. Mechanism III. The rate of (a) is given by Equation 12, for (e) by Equation 17 and for (g) by

$$v_g = k_g^e \theta_{OH} c_s \exp(\alpha_g f \eta) \qquad (25)$$

From Equations 17 and 25 it follows

$$\frac{v_g}{v_e} = \frac{k_g^e}{k_e^e} c_s \exp\{(\alpha_g - \alpha_e) f \eta\} \qquad (26)$$

Since $i_g = Fv_g$, $i_e = Fv_e$, $i_{O_2} = 4i_e$ and $i_{ClO_4} = 2i_g$ the ratio of the current densities or the current efficiencies for perchlorate and oxygen formation is

$$\frac{i_{ClO_4}}{i_{O_2}} = \frac{\Gamma_{ClO_4}}{\Gamma_{O_2}} = \frac{2k_q^e}{k_e^e} c_s \exp\{(\alpha_g - \alpha_e) f \eta\} \qquad (27)$$

At steady state

$$i_a = i_e + i_g \qquad (28)$$

and

$$i = 4i_e + 2i_g \qquad (29)$$

It can be shown that if (a) is the rate-determining step, the slope of the $\eta/\ln i_a$ curve is $(\alpha_a f)^{-1}$ where $i_a = 0.25 i_{O_2} + 0.5 i_{ClO_4}$. Moreover, from Equation 27 it follows that the slope of the $\eta/\ln(\Gamma_{ClO_4}/c_s\Gamma_{O_2})$ curve is $((\alpha_g - \alpha_e) f)^{-1}$ at a constant c_b.

5.2.4. Mechanism IV. The rates of (a) and (g) are given by Equations 12 and 25, respectively, and that of (h) by

$$v_h = k_h \theta_{OH}^2 \qquad (30)$$

From Equations 25 and 30 it follows that

$$\frac{v_g}{v_h} = \frac{k_g^e c_s}{k_h \theta_{OH}} \exp(\alpha_g f \eta) \qquad (31)$$

At steady state

$$v_a = v_g + v_h \qquad (32)$$

From Equations 31 and 32

$$\left(\frac{2v_h}{v_g} + 1\right)^2 - 1 = \frac{4k_h k_a^e}{(k_g^e c_s)^2} \exp\{(\alpha_a - 2\alpha_g) f \eta\} \qquad (33)$$

It can be shown that $i_{ClO_4} = 2Fv_g$ and $i_{O_2} = Fv_h$ (i.e., $v_{O_2} = \frac{1}{4} v_h$ and $i_{O_2} = 4Fv_{O_2}$). Furthermore, $\Gamma_{ClO_4} = i_{ClO_4}/i$ and $\Gamma_{O_2} = i_{O_2}/i$. From Equation 33 there follows a relation between Γ_{O_2} and Γ_{ClO_4}.

$$\left(\frac{4\Gamma_{O_2}}{\Gamma_{ClO_4}} + 1\right)^2 - 1 = \frac{4k_h k_a^c}{(k_g^e c_s)^2} \exp\{(\alpha_a - 2\alpha_g) f \eta\} \qquad (34)$$

Table 1 shows that the possible rate-determining step is (a). Since $i_a = i - 0.5 i_{ClO_4}$ the Tafel slope of the $\eta/\ln(i - 0.5 i_{ClO_4})$ curve is $(\alpha_a f)^{-1}$. From Equation

34 it follows that the slope of $\eta/\ln(((4\Gamma_{O_2}/\Gamma_{ClO_4}) + 1)^2 - 1)$ curve is $((\alpha_a - 2\alpha_g)f)^{-1}$ at constant c_b.

6. Discussion

6.1. *Mechanism for perchlorate formation*

The mass transfer coefficient for chlorate in the absence of oxygen evolution, $k^m_{F,ch}$ was determined indirectly with the use of $Fe(CN)_6^{4-}$ as indicator ion. It was found that in 1.64 *m* $NaClO_4$ and at 323 K $k^m_{F,Ch} = 1.98 \times 10^{-5} u_s^{0.66}$ m s^{-1}, where u_s is expressed in m s^{-1} [11]. The mass transfer coefficient for ClO_3^- in the presence of oxygen evolution, $k^m_{FB,ch}$, was determined as a function of the rate of oxygen evolution for solutions containing 1.64 *m* $NaClO_4$ and small concentrations for $NaClO_3$ and at 323 K and a flow rate of 0.06 m s^{-1}.

For this series of experiments useful experimental data for $k^m_{FB,ch}$ were only obtained at $i_{O_2} >$ 1 kA m^{-2}. These data are given by $k^m_{FB,ch} = 8.0 \times 10^{-5} i_{O_2}^{0.85}$ m s^{-1}, where i_{O_2} is expressed in kA m^{-2} [11].

Various empirical correlations have been proposed to calculate the mass transfer coefficient k^m_{FB} for a gas-evolving electrode in combined forced and bubble-induced solution flow [12]. The correlation $(k^m_{FB})^2 = (k^m_F)^2 + (k^m_B)^2$ is suitable for calculation of k^m_{FB} from the single mass transfer coefficients k^m_F and k^m_B [13]. Taking into account the viscosity, the solution density and the mass transfer due to ionic migration and assuming the bubble behaviour does not depend on the composition of the $NaClO_3$–$NaClO_4$ solution, the overall mass transfer coefficient for chlorate, $k^m_{FB,ch}$, has been calculated as a function of i_{O_2} and u_s for various $NaClO_3$–$NaClO_4$ solutions. Detailed results have been published in [11].

The chlorate concentration at the anode surface, c_s, during electrolysis is of great interest and has been calculated for relevant series of electrolyses. Some calculation results are given in Fig. 9 for electrolyses with solutions containing 1.64 *m* $NaClO_4$ and various concentrations of $NaClO_3$. This figure shows that in some cases the calculated c_s is even negative. This means that $k^m_{FB,ch}$ used is too small.

The series of electrolyses with a 3.76 *m* $NaClO_3$ + 1.64 *m* $NaClO_4$ and at a high solution flow rate (i.e., 0.33 m s^{-1}) is used as a first check of the mechanism, since the concentration difference $c_b - c_s$ is the smallest for this series. To determine the transfer coefficient for the first step of the water oxidation, the potential is plotted against

$$\ln i_{O_2}, \quad \ln(i - 0.75 i_{O_2} - 0.5 i_{ClO_4}),$$
$$\ln(0.25 i_{O_2} + 0.5 i_{ClO_4}) \quad \text{and} \quad \ln(i - 0.5 i_{ClO_4})$$

for mechanisms I, II, III and IV, respectively, in Fig. 10.

The experimental data have been taken from Figs 5 and 8. From the slope of the straight line, the transfer coefficient α_a has been calculated. The results for the various mechanisms are given in Table 2.

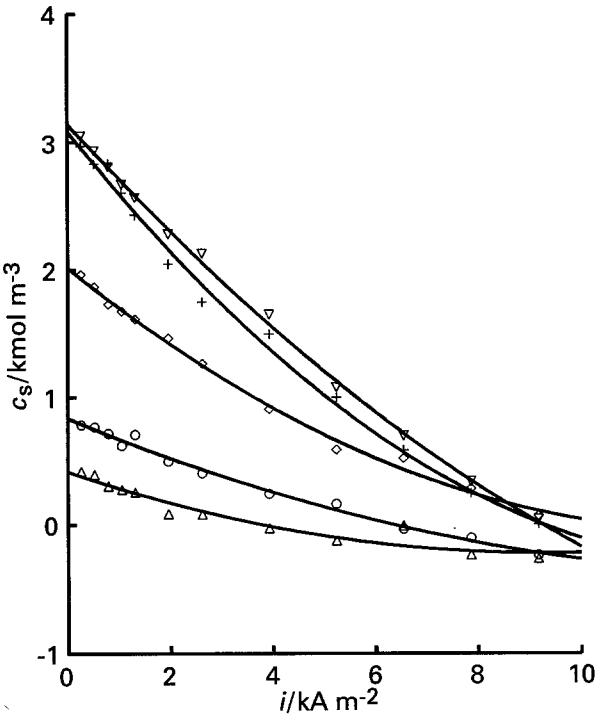

Fig. 9. Chlorate concentration at platinum anode surface as a function of current density for electrolyses in solutions containing 1.64 *m* $NaClO_4$ and various concentrations of $NaClO_3$: (△) 0.47 *m*, (○) 0.94 *m*, (◇) 2.35 *m* and (+) 3.76 *m* $NaClO_3$ at a solution flow rate of 0.06 m s^{-1} and in 1.64 *m* $NaClO_4$ + 3.76 *m* $NaClO_3$ (▽) at a solution flow rate of 0.33 m s^{-1}. Temperature: 50° C.

The transfer coefficient for the first step of chlorate oxidation has been obtained by plotting in Fig. 11 the potential as a function of $\ln(i_{ClO_4}/2c_s)$ for mechanisms I and II, $\ln(i_{ClO_4}/c_s i_{O_2})$ for mechanism

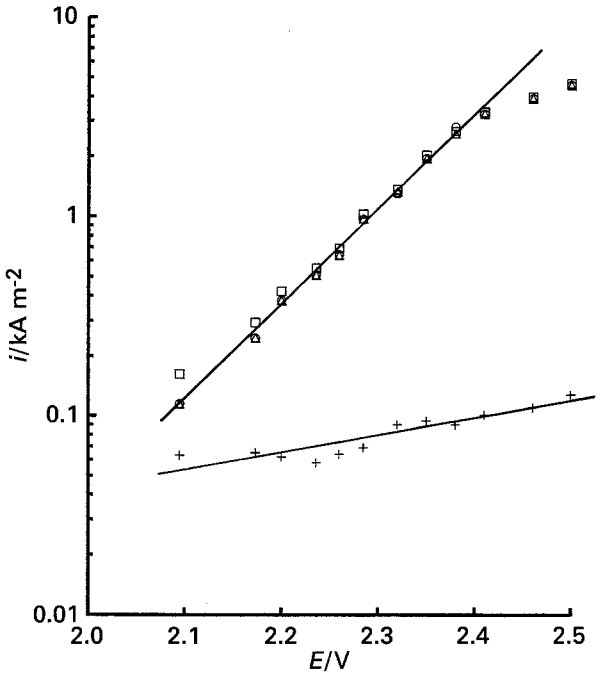

Fig. 10. Electrode potential plotted against $\ln i_a$ for an electrolysis at a platinum anode in a solution containing 3.76 *m* $NaClO_3$ + 1.64 *m* $NaClO_4$ and at 50° C and a solution flow of 0.33 m s^{-1}, where $i_a = i_{O_2}$ (+), $i - 0.5 i_{ClO_4} - 0.75 i_{O_2}$ (△), $0.5 i_{ClO_4} + 0.25 i_{O_2}$ (○) and $i - 0.5 i_{ClO_4}$ (□) for mechanism I, II, III and IV, respectively.

Table 2.

Mechanism	*Experimental transfer coefficients*	*Slope q*	
		Theoretical	*Experimental*
I	$\alpha_a = 0.13$ $\alpha_b = 0.35$	1 for (13)	1.3 ± 0.1
II	$\alpha_a = 0.32$ $\alpha_b = 0.35$	1 for (22)	$\approx 0 \pm 0.1$
III	$\alpha_a = 0.32$ $\alpha_g - \alpha_e = 0.38$	1 for (27)	2.0 ± 0.3
IV	$\alpha_a = 0.28$ $\alpha_g = 0.37$	−2 for (34)	-1.9 ± 0.3

III and

$$\ln\left(c_s^2\left(\left(\frac{4i_{O_2}}{i_{ClO_4}}+1\right)^2-1\right)\right)$$

for mechanism IV.

The experimental data for E and Γ_{ClO_4} are taken from Figs 5 and 8 and those for c_s from Fig. 9. Moreover, $i_{ClO_4} - \Gamma_{ClO_4}$ and $i_{O_2} = i - i_{ClO_4}$.

To show the effect of the increase in the difference $c_b - c_s$ with increasing potential on the Tafel slope, in Fig. 11 the potential is also plotted against $\ln(i_{ClO_4}/c_s i_{O_2})$. From Fig. 11, it follows that the slope of the $E/\ln(i_{ClO_4}/2c_s)$ and that of the $E/\ln(i_{ClO_4}/2c_b)$ curve are practically the same in the potential range from 2.1 to 2.35 V.

At high potentials, that is, at high current densities, the effect of the chlorate concentration on the Tafel slope is large. It may be concluded that the calculated decline of c_s with increasing current density is too high. The calculated c_s is very sensitive to the mass transfer coefficient for ClO_3^- ions and the contribution of ClO_3^- ions to the migration current. The mass transfer coefficient for ClO_3^- ions for the $NaClO_3$–$NaClO_4$ solution of Fig. 11, has not been determined directly, but obtained from an electrolysis with a small $NaClO_3$ concentration and taking into account differences in kinematic viscosity and solution velocity. From Fig. 11 it can be concluded that the effect of decrease in c_s is 'overcompensated'. It may be possible to obtain from Fig. 11 a more correct value for c_s at high potentials or current densities.

From the solid lines of Fig. 11 α_b for mechanisms I and II, $\alpha_g - \alpha_e$ for mechanism III and α_g for mechanism IV can be obtained, respectively. The results are given in Table 2. Electrolyses in $NaClO_3 + NaClO_4$ solutions with 1.64 *m* $NaClO_4$ and various $NaClO_3$ concentrations were carried out. Experiments where the calculated c_s is very small, or even negative, are left out of consideration.

To elucidate the mechanism $(\Gamma_{ClO_4}/\Gamma_{O_2})\exp\{-(\alpha_b - \alpha_a)f(E-2.0)\}$, $[2\Gamma_{ClO_4}/(2\Gamma_{ClO_4}+\Gamma_{O_2})]\exp\{-(\alpha_b-\alpha_a)f(E-2.0)\}$ and $(\Gamma_{ClO_4}/\Gamma_{O_2})\exp\{-(\alpha_g-\alpha_e)f(E-2.0)\}$ at various current densities for mechanisms I–III, respectively, are plotted against c_s on logarithmic scales in Fig. 12, and $\{[(4\Gamma_{O_2}/\Gamma_{ClO_4})+1]^2-1\}\exp\{-(\alpha_a-2\alpha_g)f(E-2.0)\}$ at various current densities for mechanism IV are

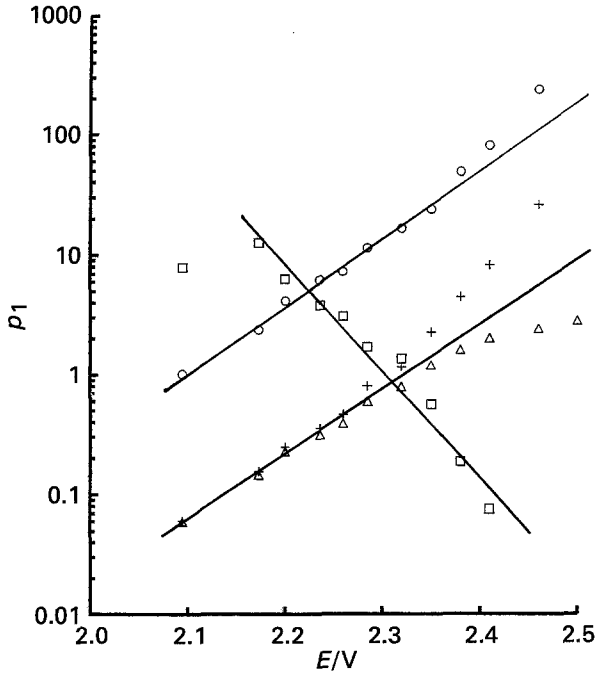

Fig. 11. Electrode potential against $\ln p_1$ for electrolysis at a platinum anode in solution containing 3.76 *m* $NaClO_3$ + 1.64 *m* $NaClO_4$ at 50° C and a solution flow of 0.33 m s^{-1}, where $p_1 = i_{ClO_4}/2c_s$ (+) and $i_{ClO_4}/2c_b$ (△) for mechanisms I and II, $p = i_{ClO_4}/c_s i_{O_2}$ for mechanism III (○), and $c_s^2\{[(4i_{O_2}/i_{ClO_4})+1]^2-1\}$ for mechanism IV (□) and i_{O_2} and i_{ClO_4} are given in kA m^{-2} and c_s and c_b in kmol m^{-3}.

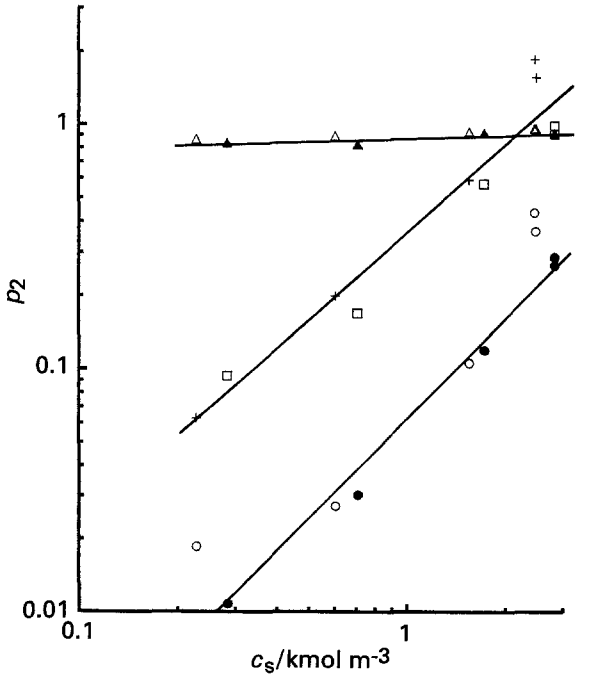

Fig. 12. Parameter p_2 against c_s on a double logarithmic scale for electrolyses at a platinum anode in a solution containing 1.64 *m* $NaClO_4$ and various $NaClO_3$ concentrations, and at 50° C and a solution flow rate of 0.06 m s^{-1}, where p_2 is $(\Gamma_{ClO_4}/\Gamma_{O_2})\exp\{-(\alpha_b-\alpha_a)f(E-2.0)\}$ at $i = 0.79$ (□) and 1.31 kA m^{-2} (+), $[2\Gamma_{ClO_4}/(2\Gamma_{ClO_4}+\Gamma_{O_2})]\exp\{-(\alpha_b-\alpha_a)f(E-2.0)\}$ at $i = 0.79$ (▲) and 1.31 kA m^{-2} (△), $(\Gamma_{ClO_4}/\Gamma_{O_2})\exp\{-(\alpha_g-\alpha_e)f(E-2.0)\}$ at $i = 0.79$ (●) and 1.31 kA m^{-2} (○), for the mechanisms I–III.

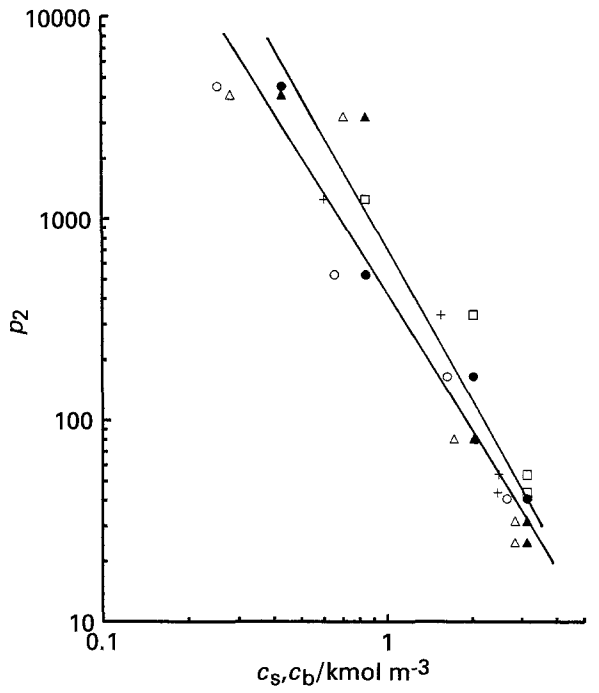

Fig. 13. Parameter p_2 against c_s and c_b on a double logarithmic scale for electrolyses at a platinum anode in solution containing 1.64 *m* $NaClO_4$ and various $NaClO_3$ concentrations at 50° C and a solution flow rate of 0.06 m s^{-1}, where $p_2 = 10^{-2}\{[(4\Gamma_{O_2}/\Gamma_{ClO_4}) + 1]^2 - 1\} \exp(-(\alpha_a - \alpha_g) f(E - 2.0))$ at c_b and at $i = 0.79$ (▲), 1.05 (●) and 1.31 kA m^{-2} (□), for mechanism IV.

plotted against c_s and c_b on a double logarithmic scales in Fig. 13. The slope q of the linear $\log p_2/\log c_s$ lines from Figs 12 and 13 are given in Table 2.

From Table 2 it follows that based on the results for the transfer coefficient for the first step of the water oxidation, viz. reaction (a), and on the comparison between the theoretical and the experimental slopes, the formation of perchlorate by oxidation of chlorate occurs according to mechanism IV. This means that the formation of an adsorbed hydroxyl radical by oxidation of water is the first step in the overall electrode reaction. The hydroxyl radicals either combine to produce an adsorbed oxygen atom or take part in an electrochemical oxidation step with chlorate ions to produce perchlorate ions.

Figure 3 shows a limiting current-density region where the limiting current density decreases with increasing salt concentration. A similar result has been obtained for platinum electrodes in concentrated perchloric acid solutions and it is suggested that adsorption of perchlorate ions is believed to be the cause of the limiting current [14]. The transition range between the upper and lower Tafel lines begins at a potential decreasing slightly with increasing perchloric acid concentration and finishes at a potential decreasing strongly with increasing perchloric acid concentration. The overvoltage of the upper Tafel curves decreases with increased perchloric acid concentration at a given current density. Similar results have been obtained from a sodium chlorate electrolysis on a platinum electrode [15].

Analogously to an electrolysis of a perchlorate solution [14], it is assumed that for an electrolysis of chlorate the point of inflection of the curve connecting the upper and lower Tafel lines represents the point where chlorate ion discharge begins. The potential of the inflection point is much higher for perchlorate solution than for a chlorate solution [15] and the current density for oxygen evolution at the inflection potential is much higher for a perchlorate solution than for a chlorate solution (Fig. 3). This means that for a perchlorate + chlorate solution under the applied conditions the discharge of perchlorate as the first step in the formation of oxygen [14] can be discounted.

The shape of the polarization curve may be related to the stages of oxidation of the platinum electrode surface. A schematic picture of the chemical state of a platinum electrode surface in 0.5 *m* H_2SO_4 at 25° C as a function of the applied potential is proposed by Peuckert *et al.* [10]. Since the total polarization curve in acidic sulphate solution [16] is similar to that in chlorate solution (Fig. 2), where the pH of the solution at the oxygen-evolving electrode is relatively low, depending on the current density, it is likely that in chlorate and sulphate solutions the chemical state of the platinum anode surface is similar. The platinum electrode surface in the upper Tafel region is covered completely by a multilayer of $Pt(OH)_4$ and that in the lower Tafel region partly by a monolayer of $Pt(OH)_4$ [10].

From Fig. 3 it follows that the rate of discharge of H_2O in the lower Tafel region is hindered by the presence of $Pt(OH)_4$ on the electrode surface. This hindering results in a limiting current for the H_2O discharge in the transition range.

It has been found that the current density at the inflection potential in the transition range depends strongly on the concentration and the nature of the dissolved anion (Fig. 3). The difference in the activity of water for the chlorate and the perchlorate solutions from Fig. 3 is small. The water activity has been obtained from the osmotic coefficients of the electrolytes [17]. Consequently, the water activity has no significant effect on the current density at the inflection potential. It is possible that $Pt(OH)_4$ layer on the electrode surface affects the adsorption of anions like chlorate and perchlorate. This adsorption inhibits oxygen evolution from water discharge and affects the current density at the inflection potential. Thus, the presence of the multilayer of $Pt(OH)_4$ is of great interest for the oxidation of chlorate to perchlorate. The remarkable result shown in Fig. 2 supports this suggestion.

References

[1] N. Ibl and H. Vogt, *in* 'Comprehensive Treatise of Electrochemistry', vol. 2 (edited by J. O'M Bockris, B. E. Conway, E. Yeager and R. E. White), Plenum Press, New York and London (1981) p. 208.
[2] J. C. Grigger, H. C. Miller and F. D. Loomis, *J. Electrochem. Soc.* **105** (1958) 100.
[3] A. Legendre, *Chem. Ing. Techn* **34** (1962) 379.

[4] N. Munichandraiah and S. Sathyanarayana, *J. Appl. Electrochem.* **17** (1987) 33.
[5] O. de Nora, P. Gallone, C. Traini and G. Meneghini, *J. Electrochem. Soc.* **116** (1969) 146.
[6] L. R. Czarnetzki and L. J. J. Janssen, *J. Appl. Electrochem.* **22** (1992) 315.
[7] L. C. Czarnetzki, Thesis, Eindhoven, University of Technology (1989).
[8] J. P. Hoare, *in* 'Encyclopedia of Electrochemistry of the Elements', vol. II, (edited by A. J. Bard), Marcel Dekker, New York (1974) p. 275.
[9] K. I. Rozental' and V. Veselovskii, *Dokl. Akad. Nauk. SSSR* **111** (1956) 637.
[10] M. Peuckert, F. P. Coenen and H. P. Bonsel, *Electrochim. Acta* **29** (1984) 1305.
[11] P. D. L. van der Heyden, Report, Eindhoven (1992).
[12] H. Vogt, *in* 'Comprehensive Treatise of Electrochemistry', vol. 6, (edited by E. Yeager, J. O'M Bockris, B. E. Conway and S. Sarangapanic), Plenum Press, New York and London (1983) p. 455.
[13] L. J. J. Janssen, *J. Appl. Electrochem.* **17** (1989) 1177.
[14] T. R. Beck and R. W. Moulton, *J. Electrochem. Soc.* **103** (1956) 247.
[15] K. Sugino and S. Aoyagi, *ibid.* **103** (1956) 166.
[16] S. J. Zhadanov, *in* 'Encyclopedia of Electrochemistry of the Elements', vol. IV, (edited by A. J. Bard), Marcel Dekker, New York (1975) p. 343.
[17] R. A. Robinson and R. H. Stokes, 'Electrolyte Solutions', Butterworths, London, 2nd edn (1959) p. 483.